Tight-binding molecular dynamic study of silver clusters

Jijun Zhao [*]

Department of Physics and Astronomy, University of North Carolina at Chapel Hill, Chapel Hill, NC 27599, USA.
International Centre for Theoretical Physics, P.O.Box 586, Trieste 34100, Italy

(April 29, 2019)

Tight-binding molecular dynamics (TBMD) is used to study the structural and electronic properties of silver clusters. The ground state structures of Ag clusters up to 21 atoms are optimized via TBMD combined with genetic algorithm (GA). The detailed comparison with *ab initio* results on small Ag_n clusters ($n = 3 - 9$) proves the validity of the tight-bind model. The clusters are found to undergo a transition from "electronic order" to "atomic order" at $n = 10$. This is due to s-d mixing at such size. The size dependence of electronic properties such as density of states (DOS), s-d band separation, HOMO-LUMO gap, and ionization potentials are discussed. Magic number behavior at Ag_2, Ag_8, Ag_{14}, Ag_{18}, Ag_{20} is obtained, in agreement with the prediction of electronic ellipsoid shell model. It is suggested that both the electronic and geometrical shell exist in the coinage metal clusters and they play a significant role in determining cluster properties.

36.40.Cg, 36.40.Mr, 71.24.+q

I. INTRODUCTION

The structural and electronic properties of metal clusters are currently a field of intensive research both theoretically and experimentally[1−3]. The basic theoretical concept in the electronic structure of alkali metal clusters is the shell model based on jellium sphere (or ellipsoid) approximation[1,2], which has successfully interpreted the magic number effect in Na_n and K_n clusters ($n =$2, 8, 20, 40, $\cdots$). As compared to alkali-metal clusters, the application of electronic shell model to coinage-metal clusters (Cu_n, Ag_n, Au_n) is somewhat questionable due to the existence of inner d electrons. Among the noble metal clusters, Ag_n is expected to exhibit the largest similarity to the alkali metal clusters as the $4d$ orbitals in Ag atom are low-lying and act almost like innershell core orbitals. Experimental studies on silver clusters include mass-spectra[4], ionization potentials (IPs)[5,6], photoelectron spectra[7−9], electron spin resonance (ESR)[10], optical resonance absorption[11], etc. In general, most of the cluster properties resemble the predictions of shell model within one s electron picture. But there are still some experimental evidences for Ag_n that are different from alkali-metal clusters and cannot be understood via the shell model of s electrons. For instance, the Mie resonance peak of silver clusters exhibit blue shift with decreasing cluster radius[11], while red shift of Mie resonance frequency is found for alkali-metal clusters. A direct comparison of photoelectron spectra between Ag_n and Na_n display significant difference that might be attributed to the d orbitals[8]. Therefore, it is important to clarify the contribution of $4d$ electrons and $s - d$ interaction in the silver clusters and the geometrical effect on the electronic properties of the clusters.

Besides shell model, the metal clusters have been investigated by accurate quantum chemical approaches based on molecular orbital theory[3]. However, such *ab initio* calculations on coinage metal clusters are quite time consuming and limited in small size[12−15]. Among those works, the most detailed and comprehensive study of small neutral silver clusters (Ag_2 to Ag_9) has been performed via configuration interaction (CI) method with relativistic effective core potential (RECP)[14]. On the other hand, the electronic structures of several larger silver clusters has been approximately described by a modified Hückel model[16]. However, all these studies are carried out for limited number of structural candidates with symmetry constrain. An unbiased minimization for the cluster ground state structure incorporated with electronic structure calculations would be much more informative for understanding the interplay between geometrical and electronic structure and testing the validity of electronic shell model.

Up to now, the most reliable and accurate procedure in dynamic searching of cluster equilibrium geometries is provided by Car-Parrinello (CP) method with simulated annealing (SA)[17]. But such kind of *ab initio* simulation is also limited in small size (about $n \leq 10$) in a truly global optimization because of the rapidly increase in computational expense with cluster size. Among coinage metal clusters, the CP method has been employed to study small Cu_n clusters ($n = 2 - 10$) recently[18], but the corresponding investigation on silver and gold clusters is not available so far. In recent years, tight-binding molecular dynamics has been developed as an alternative to CP method in atomistic simulation for larger scaled systems[19]. As compared to *ab initio* methods, the parameterized tight-binding (TB) Hamiltonian reduces the computational cost dramatically. It is more reliable than classical simulation based on empirical potential since the atomic motion is directly coupled with electronic structure calculation at each steps. For transition-metal clusters, M.Menon and co-workers have proposed a minimal parameter tight-binding scheme and used it to study nickel and iron clusters[20,21]. In this work, we shall introduce a similar TB model for silver. By using the

TBMD as a local minimization approach, genetic algorithm (GA)[22−25] is employed to search the global minimal structure of Ag_n clusters up to 21 atoms. The size dependence of relative stabilities, density of states (DOS), HOMO-LUMO gaps, and ionization potentials of the clusters are calculated and compared with available experimental results. The magic effect of electronic shell and the interplay between geometrical and electronic structure in silver clusters are discussed.

II. THEORETICAL METHOD

In the minimal parameter tight-binding scheme proposed by M.Menon et al.[20], the total binding energy E_b of transition-metal atoms is written as a sum:

$$E_b = E_{el} + E_{rep} + E_{bond}. \tag{1}$$

E_{el} is the electronic band structure energy defined as the sum of one-electron energies for the occupied states

$$E_{el} = \sum_k^{occ} \epsilon_k \tag{2}$$

where energy eigenvalues ϵ_k can be obtained by solving orthogonal $9n \times 9n$ TB Hamiltonian including $4d$, $5s$ and $5p$ electrons. The repulsive energy E_{rep} is described by a pair potential function $\chi(r)$ of exponential form:

$$E_{rep} = \sum_i \sum_{j>i} \chi(r_{ij}) = \sum_i \sum_{j>i} \chi_0 e^{-4\alpha(r-d_0)} \tag{3}$$

where r_{ij} is the separation between atom i and j, $d_0 = 2.89$Å is the bond length for the fcc bulk silver[26], α is taken to be one-half of $1/d_0$ according to Ref.20.

In order to reproduce the cohesive energies of small clusters through bulk TB hopping parameters, it is still necessary to introduce a bond-counting term E_{bond}:

$$E_{bond} = -N[a(n_b/N) + b] \tag{4}$$

Here the number of bonds n_b are evaluated by summing over all bonds according to cutoff distance R_c

$$n_b = \sum_i [\exp(\frac{d_i - R_c}{\Delta}) + 1]^{-1}. \tag{5}$$

It should be noted that only the first two terms E_{el} and E_{rep} in Eq.(1) contribute to the interatomic forces in TBMD simulation, while the E_{bond} term is added after the relaxation has been achieved. However, for metal clusters, this correction term is significant in distinguishing various isomers at a given cluster size[20].

The $9n \times 9n$ TB Hamiltonian matrix is constructed with Slater-Koster scheme, while the distance scaling of hopping integrals $V_{\lambda\lambda'\mu}$ is taken as the Harrison's universal form[27]:

$$V_{\lambda\lambda'\mu}(d) = V_{\lambda\lambda'\mu}(d_0)(\frac{d_0}{d})^{\tau+2} \tag{6}$$

The parameter $\tau = 0$ for s-s, s-p, p-p interactions, $\tau = 3/2$ for s-d and p-d interaction, $\tau = 3$ for d-d interaction.

In present, we have adopted the Slater-Koster hopping integrals $V_{\lambda\lambda'\mu}(d_0)$ and the on-site orbital energy from the values fitted to first principle APW band structure calculation of bulk silver[27]. Furthermore, to transfer the on-site orbital energies levels from bulk calculation to atomic limit, a constant energy shift $\Delta\epsilon$=-15.88 eV is applied on the on-site energies from Ref.27. Such shift in on-site levels make the theoretical ionization potential of Ag_n clusters quantitatively comparable to experimental values. The repulsive potential parameter χ_0 is fitted for experimental bond length 2.48 Å of silver dimer[28]. The bond-counting terms a, b are chosen to reproduce the ab initio binding energy for small clusters Ag_3, Ag_4, Ag_5[12,14,15]. All the parameters used in our calculation are listed in Table I. These empirical parameters can describe both bulk phase and dimer of silver with an acceptable accuracy. The cohesive energy 2.75 eV, equilibrium interatomic distance 2.88 Å of fcc solid silver from TB model are close to the corresponding experimental value 2.95 eV and 2.89 Å respectively[26]. The vibrational frequency and binding energy calculated for silver dimer at equilibrium distance is 125.5 cm^{-1} and 1.25 eV, in reasonable agreement with experimental data of 192.4 cm^{-1} and 1.66 eV[29].

Table I. Parameters of TB model for silver used in this work.

ϵ_s	ϵ_p	$\epsilon_{d,xy}$	ϵ_{d,x^2-y^2}
-6.452 eV	-0.447 eV	-14.213 eV	-14.247 eV

$V_{ss\sigma}$	$V_{sp\sigma}$	$V_{pp\sigma}$	$V_{pp\pi}$	$V_{sd\sigma}$
-0.895 eV	1.331 eV	2.14317 eV	0.088 eV	-0.423 eV

$V_{pd\sigma}$	$V_{pd\pi}$	$V_{dd\sigma}$	$V_{dd\pi}$	$V_{dd\delta}$
-0.531 eV	0.207 eV	-0.429 eV	0.239 eV	-0.046 eV

d_0	α	χ_0	a	b	R_c	Δ
2.89 Å	0.692Å^{-1}	0.58 eV	-0.16 eV	0.59 eV	3.5 Å	0.1 Å

The determination of lowest energy structures of clusters is performed by a genetic algorithm (GA)[22–25]. The essential idea of this novel global optimization strategy is to mimic the Darwinian biological evolution process in which only the fittest candidate can survive. Some pioneering works have demonstrated the impressive efficiency of GA in searching the global minima of clusters as compared to standard simulated annealing. At beginning, we generate a number N_p of initial configurations by random ($N_p = 4 - 16$, depending upon cluster size). Any two candidates in this population can be chosen as parents to generate a child cluster through mating process. In the end of mating procedure, mutation operation is allowed to apply on the geometrical structure of child cluster with 30% possibility. The child cluster from each generation is relaxed by TBMD quenching of 300-500 MD steps with $\Delta t = 5 fs$. Then the locally minimized child is selected to replace its parent in the population if it has different geometry but lower binding energy. Typically, $100-150$ GA iterations is sufficient to ensure a truly global search up to $n = 21$. The detailed description about the practical operation of GA is given elsewhere[25,30].

III. STRUCTURES AND STABILITIES OF SLIVER CLUSTERS

A. Structures of small Ag_n with $n \leq 9$

By using the combined GA-TBMD strategy, we have explored the global minimal structures of Ag_n clusters up to 21 atoms. These ground state structures are shown in Fig.1 ($4 \leq n \leq 9$) and Fig.2 ($10 \leq n \leq 21$). In Table II, the structural parameters (bond lengths and bond angles), binding energies and ionization potentials of the small Ag_n clusters ($n = 3 - 9$) in ground state and some metastable structures are compared with accurate quantum chemistry calculations[12–15]. The lowest energy structures found for most of the clusters coincide well with intensive CI calculations in Ref.14 and the other works[12,13,15]. The calculated cluster properties of ground state and metastable isomers agree with *ab initio* results quantitatively. As shown in Table I, the TB bond lengths are typically within $0.05-0.15$ Å according to the *ab initio* values. The average deviation of binding energy per atom and ionization potentials from this work to *ab initio* calculations[14] is about 0.13 eV and 0.30 eV respectively.
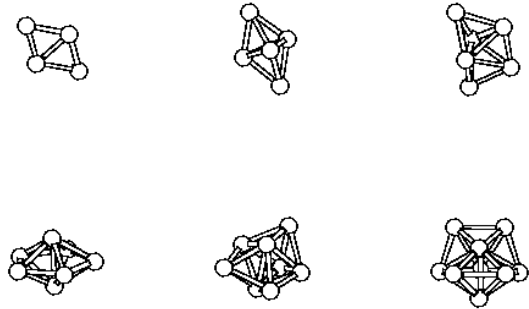

FIG. 1. Lowest-energy structures for Ag_n ($n = 4-9$) clusters.

For silver trimer, isosceles triangle is about 0.05 eV lower in energy than equilateral triangle and 0.84 eV lower than the linear isomer. ESR experiments on Ag_3[9] supports the isosceles triangle structure with C_{2v} symmetry. In the case of Ag_4, planar rhombus is lower in energy than a relaxed tetrahedron by ΔE=0.31 eV although the tetrahedron has higher coordination and has been predicted as most stable structure by using a classical many-body potential[30]. This discrepancy demonstrates the importance of incorporating the electronic structure in determining cluster geometries. The lowest energy structure found for Ag_5 is a compressed trigonal bipyramid, which has lower energy (ΔE=0.17 eV) than a planar capped rhombus. In previous studies, the planar structure has been obtained as ground state[12,14,15] but the energy difference between these two isomers is rather small (ΔE=0.31 eV in Ref.12 and ΔE= 0.003 eV in Ref.14). It is noted that the experimental ESR spectra of Ag_5 can be interpreted by a geometrical structure of deformed trigonal bipyramid. Two isoenergitic structures, a bicapped tetrahedron and a pentagonal pyramid are found for Ag_6, with ΔE=0.05 eV. The bicapped tetrahedron is more stable but this conclusion depends sensitively on the choice of empirical parameters. In Ref.14, these two structures are also found to be very close in energy ($\Delta E = 0.06$ eV) but the pentagonal pyramid is ground state. According to the theoretical HOMO-LUMO gap of these two isomers, we suggest that the bicapped tetrahedron is a better candidate since its HOMO-LUMO gap (1.05 eV) is much smaller than that obtained for pentagonal pyramid (2.67 eV), whereas experimental gap is about 0.34 eV[7]. The pentagonal bipyramid is obtained as lowest energy structure for Ag_7. The tricapped tetrahedron is a locally stable isomer with ΔE =0.48 eV, while the ΔE in Ref.14 for the same isomer is 0.41 eV. For silver octamer, a bicapped octahedron is our ground state structure, which is also found for Cu_8[18]. This near-spherical configuration can be understood by electronic shell model. The closure of electronic shell at $n = 8$ might give rise to a spherical charge density distribution, which favors the formation of spherical atomic arrangement. The tetracapped tetrahedron is predicted as metastable isomer in

Ref.14 but it is unstable upon relaxation in our simulation. Another spherical-like structure, square antiprism (D_{4d}) is found as a local stable isomer with ΔE=0.99 eV. For Ag_9, the ground state structure is a bicapped pentagonal bipyramid. Its energy is lower than that of the tricapped trigonal prism (C_{3v}) by 0.59 eV and than that of capped square antiprism (C_{2v}) by 1.01 eV. In Ref.14, bicapped pentagonal bipyramid is also found as ground state and the energy difference ΔE for the two structural isomers is 0.73 eV and 0.22 eV respectively.

Table II Comparison of structural properties (bond length, bond angle), average binding energies E_b/n, and vertical ionization potentials (IP) of small Ag_n ($n = 3 - 9$) clusters with *ab initio* calculations[12−15]. The definition of structural parameters r, α, h, etc. for smaller Ag_{3-5} clusters is chosen according to Ref.[14]; the bonds for Ag_{6-9} are defined by their lengths in Ref.[14] in a declining sequence. a denotes our present tight-binding calculation. b to e are previous *ab initio* calculations based on relativistic effective core potential configuration (RECP): b-modified coupled pair function (MCPF)[12]; c-multireference singles plus doubles configuration (MRSDCI)[13]; d-configuration interaction (CI)[14]; e-relativistic effective core potential density functional theory (RECP-DFT)[15].

	r (Å)	α (deg)	E_b/n (eV)	IP (eV)
	Ag_3, obtuse triangle (C_{2v})			
a	2.659	66.8	0.82	5.65
b	2.709	69.2	0.80	5.59
c	2.720	63.7	0.90	5.90
d	2.678	69.1	0.86	5.74
e	2.627	70.4	0.84	–

	r (Å)	α (deg)	E_b/n (eV)	IP (eV)
	Ag_4, rhombus(D_{2h})			
a	2.731	56.6	1.21	6.86
b	2.862	57.6	1.11	6.54
c	2.870	55.5	1.83	6.40
d	2.800	56.4	1.20	6.60
e	2.740	57.2	1.11	—

	r (Å)	α (deg)	$h/2$ (Å)	E_b/n (eV)	IP (eV)
	Ag_5, deformed trigonal bipyramid (C_{2v})				
a	2.749	67.5	2.34	1.38	5.88
b	2.858	65.8	2.39	1.16	—
d	2.709	67.8	2.33	1.28	5.95

	r_1 (Å)	r_2 (Å)	r_3 (Å)	r_4 (Å)	E_b/n (eV)	IP (eV)
	Ag_5, planar capped rhombus (C_{2v})					
a	2.851	2.736	2.740	2.668	1.32	6.20
b	2.842	2.842	2.842	2.842	1.22	6.18
d	2.812	2.801	2.760	2.759	1.28	6.20

	r_1 (Å)	r_2 (Å)	r_3 (Å)	r_4 (Å)	r_5 (Å)	E_b/n (eV)	IP (eV)
	Ag_6, bicapped tetrahedron (C_{2v})						
a	2.931	2.875	2.766	2.653	2.661	1.65	6.71
d	2.976	2.859	2.783	2.751	2.672	1.49	6.23

	r_1 (Å)	r_2 (Å)	E_b/n (eV)	IP (eV)
	Ag_6, pentagonal pyramid (C_{5v})			
a	2.984	2.539	1.65	7.92
d	2.828	2.740	1.50	7.00

	r_1 (Å)	r_2 (Å)	E_b/n (eV)	IP (eV)
	Ag_7, pentagonal bipyramid (D_{5h})			
a	2.879	2.858	1.87	5.95
d	2.815	2.806	1.71	5.91

	r_1 (Å)	r_2 (Å)	r_3 (Å)	r_4 (Å)	E_b/n (eV)	IP (eV)
	Ag_8, bicapped octahedron (D_{2d})					
a	3.140	2.812	2.941	2.661	2.03	7.10
d	2.973	2.812	2.804	2.735	1.80	6.80

	r_1 (Å)	r_2 (Å)	r_3 (Å)	r_4 (Å)	r_5 (Å)
	Ag_9, bicapped pentagonal bipyramid (C_{2v})				
a	2.989	2.936	2.993	2.888	2.856
d	2.934	2.887	2.881	2.836	2.786

	r_6 (Å)	r_7 (Å)	E_b/n (eV)	IP (eV)
a	2.849	2.745	2.09	5.74
d	2.766	2.752	1.77	5.10

From the above discussions for small silver clusters, we find that the agreement between TB model and *ab initio* calculations is satisfactory, particularly considering the simplicity in the present tight-binding scheme. Therefore, in the next part, we shall use this model to study larger clusters with $n \geq 10$ for which the global minimization with *ab initio* molecular dynamics is much more expensive.
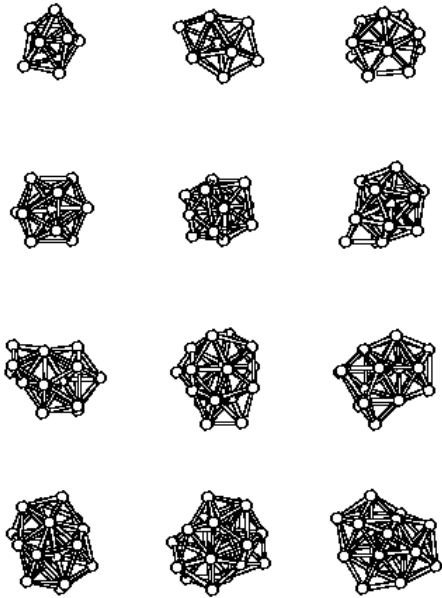
B. Structures of Ag$_n$ with $10 \leq n \leq 21$

FIG. 2. Lowest-energy structures for Ag$_n$ ($n = 10 - 21$) clusters. See text for description of structures.

The lowest energy structure of Ag$_n$ ($n = 10 - 21$) obtained from GA-TBMD simulation is shown in Fig 2. The most stable structure of Ag$_{10}$ is a deformed bicapped square antiprism (D$_{4d}$), which is similar to that found for Cu$_{10}$[18]. Starting from Ag$_{11}$, the ground state structures of Ag$_n$ clusters are based on icosahedral packing, except for Ag$_{14}$. Many other capped polyhedral structures are obtained as local isomers for Ag$_n$ with n =10-21 but it is not necessary to describe them herein. As shown in Fig.2, the structures of Ag$_{11}$, Ag$_{12}$ are the uncompleted icosahedron with lack of one or two atoms. An Jahn-Teller distorted icosahedron is then formed at Ag$_{13}$. Following the icosahedral growth sequence, the lowest energy structures of Ag$_{15}$, Ag$_{16}$, Ag$_{17}$ is the icosahedron capped with 2, 3, 4 atoms respectively. The capped single icosahedron transits into an truncated double icosahedron at Ag$_{18}$ and a complete double icosahedron at the Ag$_{19}$. Base on the double icosahedron structure, the structures of Ag$_{20}$ and Ag$_{21}$ is formed by one and two atoms capped on that of Ag$_{19}$. However, an exception occur at Ag$_{14}$,

for which we found a fcc-like packing with 4-1-4-1-4 layered structure. This ellipsoid structure is more stable than a spherical capped icosahedron structure by 0.03 eV. It is worth noted that 14 is a magic size predicted by a ellipsoid shell model[1,30].

C. Crossover from "electronic order" to "atomic order"

The concept of "particle order" (or "atomic order") and "wave order" (or "electronic order") in cluster physics[32] have been introduced in order to explain the magic number effect in the inert gas clusters with atomic shell and alkali metal clusters with electronic shell. The noble metal cluster is a mixture of the atomic core involving the relatively localized d electrons and the more delocalized s valence electrons. Therefore, it might be a intermediated system from these two extreme limit and exhibit features come from both the two orders. The equilibrium structures of small silver clusters (Ag$_3$−Ag$_9$) from our calculation are similar to those of alkali-metal clusters[3]. In contrast, the icosahedron growth sequence is obtained for clusters starting from Ag$_{11}$ that has also been found for noble gas clusters[33]. In smaller silver clusters, the 5s valence electrons are dominant in determining the cluster property and the d states are significantly lower-lying and contribute much less to the cluster bonding. Therefore, these small clusters should exhibit certain alkali-metal-like behavior in both structural and electronic aspects. As the clusters size increase, the contribution of d electrons to cluster bonding become more and more important. The bonding energy from d electrons is roughly related to the d band width[34], which is approximately proportional to the square root of the average coordination number of the clusters[35]. Consequently, the clusters tend to adopt the more compact structures such as icosahedron, which is similar to noble gas clusters[33]. The switch of structural pattern from alkali-metal like to noble gas like at around n=10 can be identified as a crossover from "electronic order" towards "atomic order" in the silver clusters. This alternation is related to the overlap of 4d and 5s electronic states which we will discussed latter. However, our further study show that the shell structure of s electrons still dominates the electronic properties such as IPs, HOMO-LUMO gaps of the silver clusters although the geometrical structures has taken "atomic order". We argue that the "electronic order" and "atomic order" can coexist in coinage metal clusters.

D. Size dependence of relative stabilities

The second differences of cluster binding energies defined by $\Delta_2 E(n) = E_b(n + 1) + E_b(n - 1) - 2E_b(n)$ is calculated and plotted in Fig.3. In cluster physics, it

is well known that the $\Delta_2 E(n)$ is a sensitive quantity which reflects the stability of clusters and can be directly compared to the experimental relative abundance. Three major characteristics can be found in the Fig.3: (i) even-odd alternation of $\Delta_2 E(n)$ with $n = 2 - 6, 15 - 21$; (ii) particular high peak at Ag_8, Ag_{18}; (iii) other maxima at odd size like Ag_{13} and Ag_{11}. The first effect can be related to the even-odd oscillation of HOMO energy and HOMO-LUMO gap in silver clusters, which is due to electron pairing effect. The articular stable clusters such as Ag_8, Ag_{18} corresponds to the magic number in electronic shell model. However, the even-odd oscillation in $\Delta_2 E(n)$ from Ag_{10} to Ag_{14} and the maximum at magic size Ag_{20} have not been observed in our calculation. In stead, some odd-sized cluster as Ag_{11}, Ag_{13} become maxima in Fig.3. These phenomena can be attributed to the geometrical effect. The closing of geometrical shell of icosahedron at Ag_{13} will enhance the stability of such clusters and reduce the relative stability of their neighboring clusters.
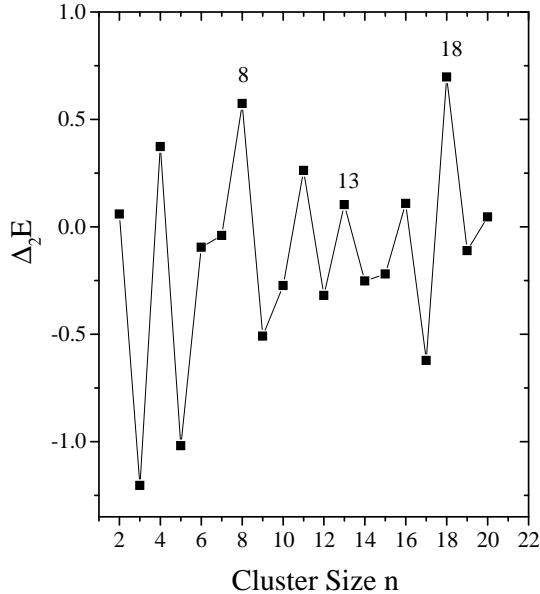

FIG. 3. Second differences of cluster binding energies $\Delta E(n) = [E_b(Ag_{n-1}) + E_b(Ag_{n+1})] - 2E_b(Ag_n)$ as a function of cluster size n for $n = 2 - 21$. Both electronic shell effect at $n = 2, 8, 18$ and geometrical shell effect at Ag_{13} can be identified. See text for details.

The simultaneous appearance of those three features in the $\Delta_2 E(n)$ demonstrates that the structure and stability of a silver cluster is determined by both electronic structure and atomic configuration. Either electronic or geometrical effect is enhanced if the corresponding shell structure is completed. This argument is supported by a

experimental probe of geometrical and electronic structure of copper clusters[36]. They found both jellium-like electronic behavior and icosahedral geometrical structure in copper clusters. In a experimental studies of mass spectra of ionized silver clusters[4], dramatic even-odd oscillation as well as substantial discontinuities at electronic magic number 8, 20 ($n = 9, 21$ for cationic clusters) are found. The discrepancy between present theoretical result and experiment may be partially attributed to the effect of ionization on the cluster stability. Since the experimental mass spectra distribution is recorded for ionized clusters Ag_n^+, it is possible that the charging on the cluster can significantly alter the geometrical and electronic structure of the cluster[3,14].

IV. ELECTRONIC PROPERTIES VS CLUSTER SIZE

A. Size evolution of electronic band

We investigated the cluster electronic properties via the electronic density of states (DOS). In Fig.4, we present the total spd electronic DOS for Ag_2, Ag_8, Ag_{13} along with bulk DOS of fcc crystal silver from TB calculation in reciprocal space. Generally, the total DOS is composed by the relatively compact d states and the more expanded sp states. In smallest clusters such as Ag_2, the d and sp bands are clearly separated. The sp states shows discrete peaks originated from symmetrical splitting of atomic orbital levels, while the d band is low-lying and considerably narrower than the bulk d band. In contrast to even-odd behavior and shell occupation of s electrons, the evolution of d states from smallest clusters towards bulk solid is a monotonic broaden of band width. As the cluster size increases, both d and sp levels gradually broaden, shift, overlap with each other, and finally come into being bulk electronic band. The DOS of Ag_8 still has molecular-like some discrete sp peaks but these electronic spectra peaks tend to overlap and form continuous band. In Ag_{13}, the sp states have developed into several subbands and the d band has overlapped with sp states. Although the DOS of Ag_{13} is roughly similar to the bulk limit, the width of d band is still considerably narrower than the bulk d band width and the fine structure of sp electronic spectra is somewhat different from bulk sp band. This fact suggests that the bulk-like behavior emerge at around Ag_{13}. We have also studied the electronic states of Ag_{55} with icosahedral and cubocta-hedral structures by using present tight-binding scheme with local minimization. The DOS for both of them are much closer to bulk band. In a previous experimental study of photoelectron spectra of silver clusters up to 60 atoms[8], it is found that the ultraviolet photoelectron spectroscopy (UPS) of smallest Ag_n, i.e., $2 \leq n \leq 10$ is different from bulk UPS and changes sensitively on cluster size. The size dependent variation of UPS for Ag_n

with $n < 10$ becomes more gradual and the UPS of Ag_{60} is already very close to that of solid silver.
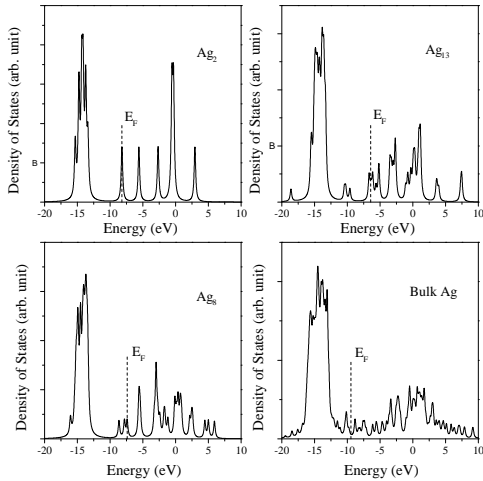

FIG. 4. Density of states (DOS) of Ag_n ($n = 2, 8, 13$) clusters vs cluster as well as bulk DOS in fcc crystalline (with Gaussian broaden of 0.02 eV).

To further clarify the size evolution of the overlap of d and sp bands in the small silver clusters, we have examined the energy separation Δ_{sd} between the highest molecular orbitals belong to d states and lowest molecular orbitals from s states. The calculated Δ_{sd} decrease rapidly from 5.20 eV for Ag_2, to 1.69 eV for Ag_5 and then to 0.10 eV for Ag_8. Finally, the d and sp band merge in Ag_n clusters with $n \geq 9$. The overlap between s and d band is believed to induce the icosahedral growth sequence starting from Ag_{11} and weaken the even-odd oscillation in HOMO-LUMO gaps and IPs of Ag_n clusters with $n > 10$. However, the overlap between sp and d states is small and the cluster HOMO is still located in the s-like electronic states. Consequently, the contribution from d electrons in Ag_n with $n > 9$ shows more importance to cluster bonding although the electronic behavior close to Fermi energy such as HOMO-LUMO gap, ionization potentials is still dominated by s orbitals.
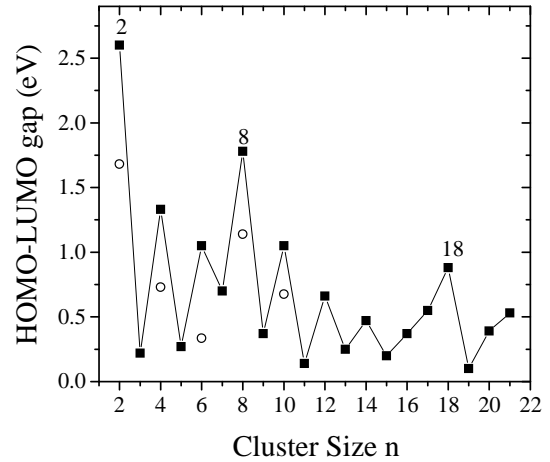
B. HOMO-LUMO gap

FIG. 5. HOMO-LUMO gap Δ (eV) vs cluster size n. The theoretical values are labeled by solid square connected with solid line and the experimental values in Ref.[7] are labeled by open circles. Electronic shell effect for $n = 2, 8, 18$ can be clearly identified.

An important electronic property of a cluster is the gap between highest occupied molecular orbital (HOMO) and lowest unoccupied molecular orbital (LUMO). In the case of magic cluster, the closure of electronic shell shall manifest itself in particularly large HOMO-LUMO gap. This effect was demonstrated experimentally for small even-sized silver and copper clusters[7] and theoretically for copper clusters[37,38]. The theoretical HOMO-LUMO gap of Ag_n ($n = 2 - 21$) along with experimental gap of small clusters Ag_n ($n = 2, 4, 6, 8, 10$)[7] are shown in Fig.5. Even-odd oscillation up to Ag_{16} as well as the particularly large HOMO-LUMO gap at Ag_2, Ag_8, and Ag_{18} are obtained. As compared to the experimental results for small Ag_n with even size, the present TB calculation has systematically overestimated the HOMO-LUMO electronic gap by about 0.5 eV. But the size dependent variation of experimental gaps and magic effect in HOMO-LUMO gaps at $n = 2, 8$ are well reproduced. The even-odd alternation for $n \geq 16$ and magic effect of Ag_{20} have not been obtained in our calculation. We suggest these are probably due to the geometrical effect, since the HOMO-LUMO gap of cluster depends sensitively on cluster structure[37]. In a previous study of

HOMO-LUMO gaps of copper clusters[37], the maxima gap at Ag_8 and Ag_{20} is found but the even-odd alternation of electronic gap and magic effect for Ag_{18} have not been obtained.

C. Ionization potential

The vertical ionization potentials (IPs) of clusters are evaluated from the highest occupied molecular orbital (HOMO) energy of neutral clusters according to Koopman's theorem. In Fig.6, the calculated IPs of Ag_n up to $n = 21$ is compared with the IP values measured by C.Jackschath[5], the prediction by metallic spherical droplet model[39], and the size dependent HOMO level (in arbitrary units) of alkali-like metal clusters by Clemenger-Nilsson ellipsoid shell model[1,31]. In comparison with experimental values in Ref.[5], the present TB calculation has almost reproduced the size dependence of IPs for silver clusters up to 21 atoms except that theoretical calculation has overestimated the IP values of some magic clusters such as Ag_2, Ag_8, and Ag_{18}. Two important size dependent behaviors are found in Fig.6: (i) dramatic even-odd alternations where clusters with even number of s valence electrons have higher IPs than their immediate neighbors; (ii) particular higher IP values at the magic clusters such as Ag_2, Ag_8, Ag_{18}, Ag_{20} and probably Ag_{14}. The even-odd variations can be attributed to electron pairing effect. Odd(even)-sized clusters have an odd(even) total number of s valence electrons and the HOMO is singly(doubly) occupied. The electron in a doubly occupied HOMO feels a stronger effective core potential since the electron screening is weaker for the electrons in the same orbital than for inner shell electrons. Therefore, the binding energy of a valence electron in a cluster of even size cluster is larger than that of odd one. It is also interesting to note that the size dependence of IPs from TB model is almost in full accordance to Clemenger-Nilsson shell model. The magic effect at Ag_2, Ag_8, Ag_{14}, Ag_{18}, and Ag_{20} predicted by electronic shell model is well reproduced even though the cluster geometries and s-d interaction has been considered. On the other hand, one can found that both the theoretical and experimental IP values for silver clusters can be roughly described by a classical electrostatic model which take the cluster as a metallic spherical droplet. This fact further suggests that the electronic behavior of silver clusters are predominantly s-like and the cluster can be approximated to be a structureless jellium sphere with shell-like electronic levels.
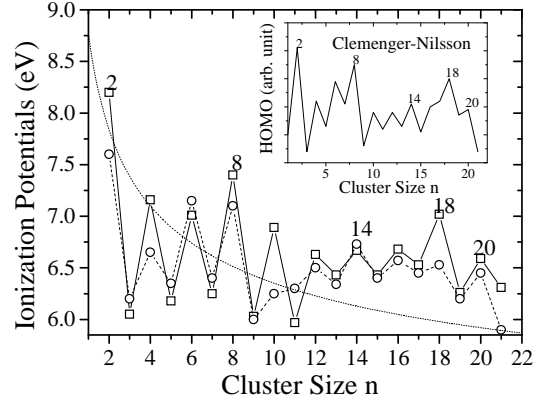

FIG. 6. Vertical ionization potentials (IPs) vs cluster size n. The measured IP values reported in Ref.[5] are labeled by open circles connected with dashed line, the theoretical values from TB calculation are labeled by open squares connected with solid line. Electronic shell closing exhibit as pronounced drops of IP at $n = 2, 8, 14, 18, 20$. See text for details.

V. CONCLUSION

In conclusion, we have shown that the present TB model is able to describe the geometrical and electronic structures of silver clusters. By using a combined GA-TBMD technique, the lowest energy structures, binding energies, electronic states, s-d separation, HOMO-LUMO gap, vertical ionization potentials are obtained and compared with experiments. The main theoretical results can be summarized in the following points:

(1) The structures of small silver clusters is determined by s electrons and similar to those of alkali-metal clusters. The contribution of d electrons to cluster bonding become more important as cluster size exceed 10 atoms. The icosahedral growth pattern starts in the Ag_n with $n \geq 11$, which can be identified as "atomic order" clusters like noble gas clusters.

(2) The electronic and geometrical shell structure coexist in silver clusters and take effect in the clusters simultaneously. The electronic shell effect on cluster electronic properties has been found by present TB calculation, in which the effect of geometrical structures and d electrons are directly incorporated. The silver clusters with closed electronic shell (n =2, 8, 14, 18, 20) show more pro-

nounced electronic characteristics while the geometrical effect is enhanced as the icosahedral shell completes at Ag_{13}.

(3) Due to the pair occupation of s valence electrons on molecular orbitals, silver clusters show even-odd alternation in their relative stability, HOMO-LUMO gap, ionization potential. However, the even-odd effects can be disturbed by the sd overlap or the geometrical structures of clusters.

(4) The density of electronic states of smaller silver cluster, e.g., $n < 10$, is composed by discrete sp expanded band and a narrow d band. The bulk-like feature in DOS start at around Ag_{13} and the bulk limit can be roughly reached by $n = 55$.

The present study shows that both the geometrical and electronic effects should be considered in order to achieve a complete description of coinage clusters. Therefore, *ab initio* molecular dynamics or TBMD are essential to elucidate the interplay between geometrical and electronic structures of these clusters. The further works should include the larger clusters and extend the TB model to other transition metal elements.

[1] W.A.de Heer, Rev.Mod.Phys.**65**, 611(1993).

[2] M.Brack, Rev.Mod.Phys.**65**, 677(1993).

[3] V.Bonacic-Koutecky and L.Cespiva, P.Fantucci, J.Koutecky, J.Chem.Phys.**98**, 7981(1993).

[4] I.Katakuse, T.Ichihara, Y.Fujita, T.Matsuo, T.Sakurai, H.Matsuda, Int.J.Mass.Spectrom.In.Proc.**67**, 229(1985); **74**, 33(1986).

[5] C.Jackschath, I.Rabin, and W.Schulze, Z.Phys.D.**22**, 517(1992).

[6] G.Alameddin, J.Hunter, D.Cameron, and M.M.Kappes, Chem.Phys.Lett.**192**, 122(1992).

[7] J.Ho, K.M.Ervin, and W.C.Lineberger, J.Chem.Phys.**93**, 6987(1990).

[8] K.J.Taylor, C.L.Pettiette-Hall, O.Cheshnovsky, and R.E.Smalley, J.Chem.Phys.**96**, 3319(1992).

[9] G.F.Ganteför, H.Handschuh, H.Möller, C.Y.Cha, P.S.Bechthold, and W.Eberhardt, Surf.Sci.Lett.**3**, 399(1996); H.Handschuh, C.Y.Cha, P.S.Bechthold, G.F.Ganteför, W.Eberhardt, J.Chem.Phys.**102**, 6406(1993).

[10] J.A.Howard, R.Sutcliffe, and B.Mile, Surf.Sci.**156**, 214(1985) and reference therein.

[11] J.Tiggesbäumker, L.Köller, K.Meiwes-Broer, and A.Liebsch, Phys.Rev.A**48**, 1749(1993).

[12] C.W.Bauschlicher, Jr., S.R.Langhoff, and H.Partridge, J.Chem.Phys.**91**, 2412(1989); J.Chem.Phys.**93**, 8133(1990); H.Partridge, C.W.Bauschlicher and Jr., S.R.Langhoff, Chem.Phys.Lett.**175**, 531(1990).

[13] K.Balasurbramanian and M.Z.Liao, Chem.Phys.**127**, 313(1988); K.Balasurbramanian and P.Y.Feng, Chem.Phys.Lett.**159**, 452(1989); J.Phys.Chem.**94**, 1536(1990).

[14] V.Bonacic-Koutecky and L.Cespiva, P.Fantucci, J.Koutecky, J.Chem.Phys.**98**, 7981(1993).

[15] R.Poteau, J.L.Heully, F.Spiegelmann, Z.Phys.D**40**, 479(1997).

[16] J.Zhao, X.Chen and G.Wang, Phys.Status Solidi(b)**188**, 719(1995).

[17] V.Kumar, in *Lectures on Methods of Electronic Structure Calculations*, p.317, ed. by V.Kumar O.K.Andersen, A.Mookerjee, (World Scientific, Singapore, 1992).

[18] C.Massobrio, A.Pasquarello, R.Car, Chem.Phys.Lett.**238**, 215(1995).

[19] For a recent review, see C.Z.Wang, K.M.Ho, in *Advances in Chemical Physics*, Vol.XCIII, p.651, Ed. by I.Prigogine, S.A.Rice, (John Wiley & Sones, Inc., New York, 1996).

[20] M.Menon, J.Connolly, N.Lathiotakis, and A.Andriotis, Phys.Rev.B**50**, 8903(1994); N.Lathiotakis, A.Andriotis, M.Menon, and J.Connolly, J.Chem.Phys.**104**, 992(1996).

[21] A.Andriotis, N.Lathiotakis and M.Menon, Europhys.Lett.**36**, 37(1996); Chem.Phys.Lett.**260**, 15(1996).

[22] B.Hartke, Chem.Phys.Lett.**240**, 560(1995); S.K.Gregurick, M.H.Alexander, R.Hartke, J.Chem.Phys.**104**, 2684(1996).

[23] J.A.Niesse, H.R.Mayne, Chem.Phys.Lett.**261**, 576(1996); J.Chem.Phys.**105**, 4700(1996).

[24] D.M.Deaven, K.M.Ho, Phys.Rev.Lett.**75**, 288(1995); D.M.Deaven, N.Tit, J.R.Morris, K.M.Ho, Chem.Phys.Lett.**256**, 195(1996).

[25] Y.H.Luo, J.J.Zhao, S.T.Qiu, G.H.Wang, Phys.Rev.B**59**, 14903(1999).

[26] C.Kittle, *Introduction to Solid State Physics*, (John Wiley & Sons, New York, 1986).

[27] W.A.Harrison, *Electronic Structure and the Properties of Solids*, (Freeman, San Francisco, 1980).

[28] D.A.Papaconstantopoulos, *Handbook of the Band Structure of Elemental Solids*, (Plenum Press, New York, 1986).

[29] M.D.Morse, Chem.Rev.**86**, 1049(1986).

[30] J.J.Zhao, G.H.Wang, unpublished.

[31] S.Erkoc, Phys.Stat.Sol.(b)**161**, 211(1990).

[32] K.Clemenger, Phys.Rev.B**32**, 1359(1985).

[33] S.Bjϕrnholm, Contemp.Phys.**31**, 309(1990).

[34] J.A.Northby, J.Chem.Phys.**87**, 6166(1987).

[35] D.Tomanek, S.Mukherjee, K.H.Bennemann, Phys.Rev.B**28**, 665(1983)

[36] J.Zhao, X.Chen, G.Wang, Phys.Rev.B.50, 15424(1994).

[37] B.J.Winter, E.K.Parks, and S.J.Riley, J.Chem.Phys.**94**, 8618(1991).

[38] U.Lammers and G.Borstel, Phys.Rev.B**49**, 17360(1994).

[39] O.B.Christensen, K.W.Jacobsen, J.K.Norskov, and M.Manninen, Phys.Rev.Lett.**66**, 2219(1991).

[40] J.P.Perdew, Phys.Rev.B**37**, 6175(1988).